

1 Introduction

This report outlines a computational approach to numerically calculate the spontaneous decay lifetime of the first excited state of atomic lithium. This will be completed in a number of steps, beginning with strong assumptions on the form and potential of the atom and building to a more complex and accurate model of lithium. This is a difficult task which requires many steps as lithium is a complex, many-electron quantum system. The experimental value we wish to find numerically to within 1% accuracy is

$$\tau_{2p} \approx 27.102(7) \text{ ns.} \quad (1)$$

As outlined in the background for this task, we use atomic units ($\hbar = |e| = m_e = \sqrt{4\pi\epsilon_0} = 1, c = 1/\alpha \approx 137$). For this task, we consider the independent particle model which forms the total wavefunction from single particle wavefunctions which we decompose as

$$\psi_{nlm}(\mathbf{r}) = \frac{P_{nl}(r)}{r} Y_{lm}(\theta, \phi),$$

where $P(r)$ are the single particle radial wavefunctions. We define these wavefunctions as the eigenstates of the radial Hamiltonian,

$$H_r = \frac{-1}{2} \frac{\partial^2}{\partial r^2} - \frac{Z}{r} + \frac{l(l+1)}{2r^2} + V_{e-e}.$$

Here, V_{e-e} is the electron electron repulse term. We solve the SE by taking,

$$P(r) = \sum_j^{N_b} c_j b_j(r),$$

with $\{c_j\}$ as expansion coefficients and $\{b_j\}$ as the B-spline basis functions. Thus (using Dirac notation) the SE takes the form,

$$\sum_j \hat{H}_r |j\rangle c_j = \epsilon \sum_j |k\rangle c_j.$$

Our goal to find τ_{2p} can be achieved by first finding the spontaneous decay rate as,

$$\gamma_{ab} = \frac{2R_{ab}^2 |\omega_{ab}^3|}{3} (1.071 \times 10^{10} \text{ s}^{-1})$$

and then taking $\tau = 1/(\sum \gamma)$ where our sum extends over all lower unoccupied states. Hence for our case of the 2p orbital, we use that numerically,

$$\tau_{2p} = \left[\frac{2}{3} |\omega_{sp}|^3 \left(\int P_{2p} r P_{2s} dr \right)^2 (1.071 \times 10^{10}) \right]^{-1}.$$

We will begin with the Hydrogen Like atom assuming a Coloumb potential, then use a Green's screening potential with perturbation theory, and then use an iterative Hartree procedure and finally use a full Hartree-Fock procedure.

2 B1: Hydrogen Like

2.1 Matrix Element

We wish to consider how the Matrix element $\langle nlm|r|n'l'm'\rangle$ can be expressed in terms of the radial $P(r)$ functions where $r = |\mathbf{r}|$. This is useful to show us that we only need to consider the radial wavefunctions of the lithium atom to solve the Schrodinger equation.

$$\begin{aligned} \langle nlm|r|n'l'm'\rangle &= \int \psi_{nlm}^\dagger(\mathbf{r}) r \psi_{n'l'm'}(\mathbf{r}) r^2 \sin \theta dr d\theta d\phi \\ &= \int P_{nl}(r)^\dagger P_{n'l'}(r) r Y_{lm}^\dagger(\theta, \phi) Y_{l'm'}(\theta, \phi) \sin \theta dr d\theta d\phi \\ &= \int_0^\infty P_{nl}(r)^\dagger P_{n'l'}(r) dr \int_0^\pi \int_0^{2\pi} Y_{lm}^\dagger(\theta, \phi) Y_{l'm'}(\theta, \phi) \sin \theta d\theta d\phi \end{aligned}$$

by the integration rule of spherical harmonics with appropriate normalisation this simplifies to,

$$= \delta_{ll'} \delta_{mm'} \int_0^\infty P_{nl}(r)^\dagger P_{n'l'}(r) dr.$$

As required. This shows us that the angular part of the integral integrates out to ensure that $l = l'$ and $m = m'$ for the matrix element to be non-zero. As such, our matrix element only consists of the Radial component.

2.2 Hydrogen Like Energies

To solve the Schrodinger equation of hydrogen-like lithium, we use the B-Spline basis. We do this by left applying the state $\langle i|$ to the SE and yielding,

$$\sum_j \langle i| \hat{H}_r |j\rangle c_j = \epsilon \sum_j \langle i|j\rangle c_j,$$

which gives us the form of a generalised eigenvalue problem $Hc = \epsilon Bc$ where H, B are $N_b \times N_b$ matrices. In particular,

$$H_{ij} = \int b_i(r) \hat{H}_r b_j(r) dr = \int b_i(r) \left[\frac{-1}{2} \frac{\partial^2}{\partial r^2} + V(r) \right] b_j(r) dr = \frac{1}{2} \int b'_i(r) b'_j(r) + \int b_i(r) V(r) b_j(r) dr$$

using integration by parts. And secondly,

$$B_{ij} = \int b_i(r) b_j(r) dr.$$

To solve this numerically, we first prepare the B-Splines and their derivatives using the provided code and taking the finite difference method. Additionally, to enforce boundary conditions, when preparing the B-Splines we exclude the first 2 and the final one to ensure that the wavefunctions are 0 at $r = 0, \infty$. We set up an evenly spaced radial grid with $r_0 = 10^{-6}$ to be sufficiently small to yield accurate low energy wavefunctions and large enough to avoid numerical instability. We use 63 Bsplines (3 are removed for boundary conditions) of order 7. The rmax values and number of r values changes based on the requirements of the question. For this question we use 2501 points in our radial grid with $r_{\max} = 30$.

We can then construct the H, B matrices by definition, using the Simpson's method rule for integration. Importantly, this means we require an odd number of points in our radial grid.

We then use the DSYGV routine from LAPACK to solve the matrix problem. This gives us a set of eigenvalues (energies) and eigenvectors (c_j values which we use to construct the wavefunction). We also note that we normalise the wavefunctions to 1 before plotting and using them for further tasks.

Under these conditions, we can begin by calculating the energies for the Hydrogen-Like atom where the potential is only given by the Coloumb term $-Z/r + l(l+1)/(2r^2)$. We yield results shown in figure 1 where we compare with the theoretical hydrogen energy and find almost exact agreement until $n = 8$. In addition, we note that for each orbital, we only take the values of n which are larger than l . As we have strong agreement, we have demonstrated that the method of solving the generalised eigenvalue problem is functioning.

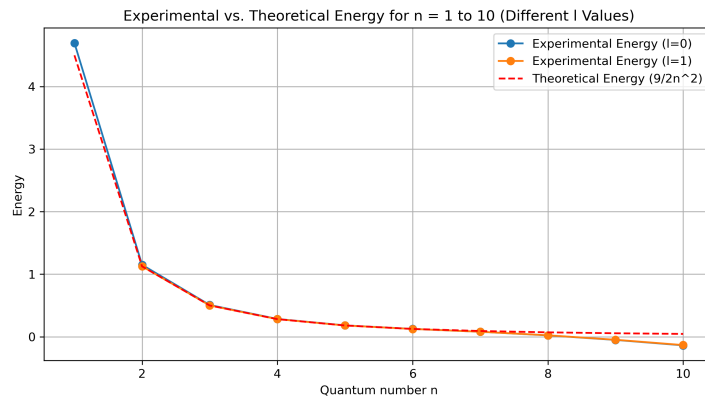


Figure 1: Comparison of experimental and theoretical energy levels for a hydrogen-like lithium atom (considering only the Coulomb potential) as a function of the principal quantum number n . The plot shows the computed energy levels for different orbital angular momentum states ($l = 0$ and $l = 1$), along with the theoretical prediction $9/2n^2$ (dashed red line). The close agreement between the numerical results and the theoretical model validates the use of the generalised eigenvalue formalism and B-Spline basis for this problem.

2.3 Radius Expectation value

To calculate the expectation value we take the integral

$$\langle r \rangle = \int P_a(r) r P_a(r) dr$$

which we solve numerically via Simpson's rule again. Doing this for the same states up to $n = 10$, we yield figure 2 where we calculate the theoretical expectation value by

$$\langle r \rangle_{nl} = \frac{a_B}{2Z} [3n^2 - l(l+1)]$$

where $a_B = 1$ is the non-dimensionalised Bohr. We clearly observe exact agreement up to $n = 6$ after which the expectation value levels out. This occurs at around $2/3 r_{max}$ indicating that when the expectation value of radius is comparable to the maximum radial coordinate, the wave functions are not given enough 'space' to increase and do not change drastically and as such, lead to a discrepancy between theory and simulation for wavefunctions as well as energy. This is the energy "problem" that arose above for $n \geq 8$.

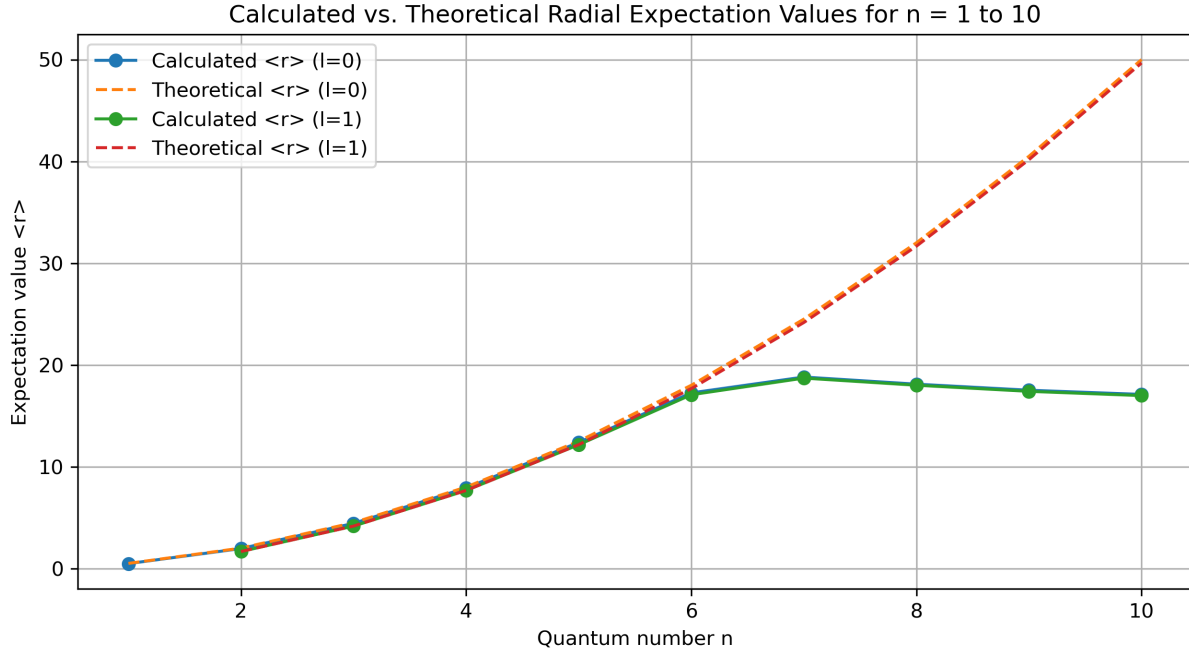


Figure 2: Comparison of calculated and theoretical radial expectation values $\langle r \rangle$ for a hydrogen-like lithium atom (considering only the Coulomb potential) as a function of the principal quantum number n . The results are shown for different orbital angular momentum states ($l = 0$ and $l = 1$), with theoretical values given by the dashed lines. There is overall good agreement, but deviations appear when r approaches approximately $\frac{2}{3} r_{max}$, leading to discrepancies in the numerical results. This deviation arises from numerical approximations for r , which become less accurate near the boundaries of the computational domain. This is also what causes the energy discrepancy in figure 1.

2.4 Radial Probability Density

Plotting the Radial probability density functions for the $1s$, $2s$ and $2p$ states allow us to see how the shape of the wavefunction changes for the orbitals and compare to other results obtained. To plot this we simply take the wavefunction squared as we always yield real wavefunction values. This gives us the plot shown in figure 3. This aligns with theory for the hydrogen atom as we expect these shapes and especially the $2p$ state to be peaked slightly earlier than the $2s$ state.

As such, under strict assumptions of hydrogen-like behaviour we are able to use our formulation of B-Splines and numerical linear algebra to calculate relevant properties of the lithium atom. However, to yield more accurate results that include inter-electron interactions in a many body quantum system fashion, we must modify our potential function.

3 B.2: Neutral Lithium: Green's Approximation

3.1 Binding Energies

As a first step to achieve this, we can approximate the repulsion potential by

$$V_{Gr}(r) = \frac{Z-1}{r} \frac{h(e^{r/d} - 1)}{1 + h(e^{r/d} - 1)}$$

where we take $h = 1$ and $d = 0.2$. We reuse the rest of the code from the previous part but increase the number of steps to 4001 and $r_{max} = 60$. We can then calculate the binding energies for the $2s$ and $2p$ valence states and plot them

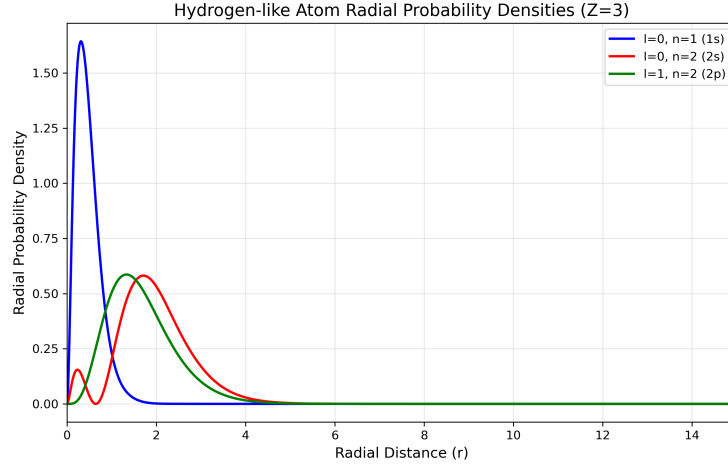


Figure 3: Radial probability densities for a hydrogen-like lithium atom ($Z = 3$), showing the spatial distributions of the 1s (blue), 2s (red), and 2p (green) orbitals. The presence of a radial node in the 2s orbital highlights the characteristic structure of excited states.

compared to experiment in 4 (see also 1). We see a rough agreement with experiment but still a large discrepancy for the 2s state. However, as a first attempt for a more accurate potential, we yield values which are far closer to experiment than the hydrogen-like atom.

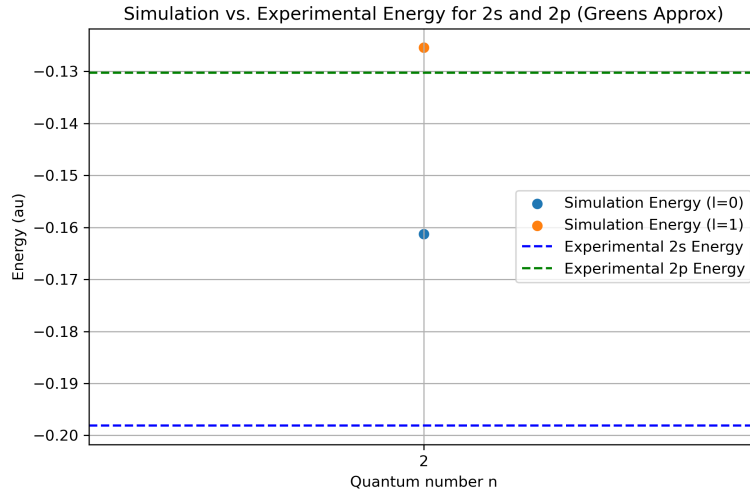


Figure 4: This plot compares simulation energies with experimental values for lithium's 2s and 2p orbitals using Greens approximation. The blue point shows the $l=0$ (2s) orbital simulation, while the orange point shows the $l=1$ (2p) orbital simulation. The horizontal dashed lines represent experimental values: blue for 2s and green for 2p. We see values on the correct order of magnitude but still fairly far away from true values.

3.2 Radial Probability Density

We can then plot the Radial probability density functions as before and yield figure 5. We see a substantially different shape for the wave functions compared to the hydrogen atom which indicates the Green's potential does indeed consider some interaction between electrons and as such changes the shape of the orbitals.

3.3 Lifetime of 2p state

To calculate the lifetime of the 2p state, we use the equations outlined above and use the value $\omega = E_{2p} - E_{2s} = 0.06791$ in our arbitrary units. We use the experimental value for this transition frequency as calculating it from our numerical simulation would use the difference in energy levels between the 2p and 2s state. This energy has been demonstrated to have fairly substantial error and hence the error of the lifetime of the 2p state would be more correlated with the error of

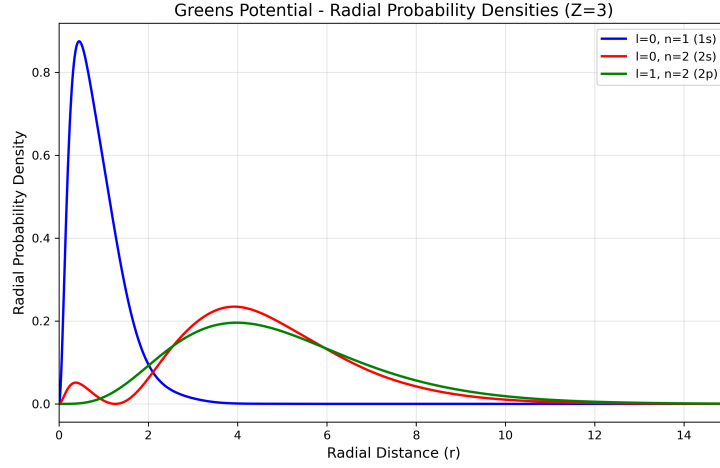


Figure 5: This graph displays the radial probability densities for different orbitals in lithium ($Z=3$) using Greens potential. The blue curve ($l=0, n=1$) shows the 1s orbital with a peak close to the nucleus. The red curve ($l=0, n=2$) represents the 2s orbital with its characteristic node. The green curve ($l=1, n=2$) shows the 2p orbital, which has zero probability at the nucleus and extends farther from the nucleus.

the energy levels than the wavefunctions. Additionally, the frequency is cubed and so the error from using the simulated transition frequency would propagate and blow out any accuracy from the wavefunctions.

This gives us the value 19.7726 ns which has an error of 27% compared to the experimental value. Regardless, having this value in the right order of magnitude indicates that our approximation is yielding values which are reasonable and close to the true value, but we still approximate away much of the true interactions occurring within the atom.

3.4 Perturbation Theory

To use the Green's potential to get a closer approximation for the energies of the 2s and 2p states, we can use a first order perturbation theory. The full details of this are in the task sheet but in short we can calculate the first order change in energy by

$$\delta\epsilon_a = \langle \delta V \rangle_a = \langle V_{ee} \rangle_a - \langle V_{Gr} \rangle_a$$

where

$$\langle V_{Gr} \rangle_a = \int |P_a(r)|^2 V_{Gr}(r) dr$$

and

$$\langle V_{ee} \rangle_a = 2 \int y_{1s,1s}^0(r) |P_a(r)|^2(r) dr$$

where

$$y_{a,b}^k = \int P_a(r') P_b(r') \frac{r_{<}^k}{r_{>}^{k+1}} dr'.$$

Using the given y_{kab} function, we can evaluate these by saving the 1s wavefunction and then calculate the perturbations for the 2s and 2p states. Including the perturbations gives us the energies shown in 6. We clearly see a much stronger agreement with theory suggesting that perturbation theory is useful in correcting our energies and allowing us to yield more accurate energies even with the simple greens screening potential. The form for the perturbation of V_{ee} term, suggests that we should perhaps use the y_{kab} function in the potential in some capacity. This leads us to the Hartree procedure.

4 B.3: Self-Consistent Hartree Procedure

4.1 Hartree Procedure Convergence

To implement the Hartree procedure we replace the Greens potential with the Hartree/Direct potential given by

$$V_{Dir}(r) = 2y_{1s,1s}^0(r)$$

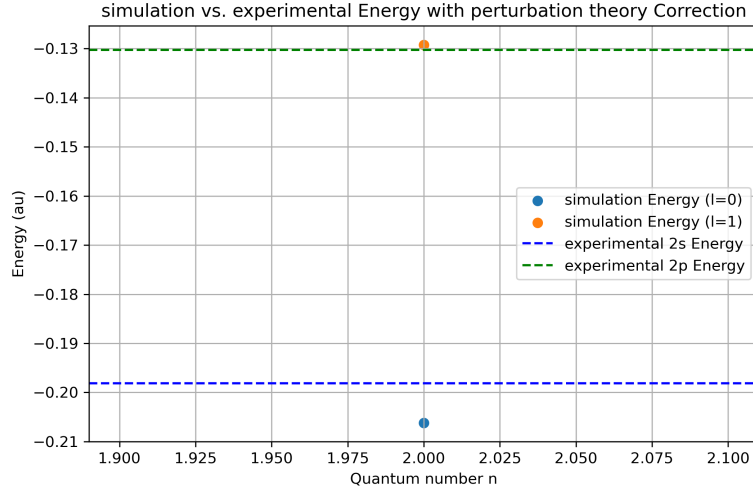


Figure 6: This plot shows improved energy calculations after applying perturbation theory corrections. The blue point ($l=0$) is much closer to the experimental 2s value. The orange point ($l=1$) matches almost exactly with the experimental 2p energy. This demonstrates how even first order perturbation theory improves the accuracy of the computational model.

which suggests that we should start with some initial potential, find the 1s wavefunction and then redefine the potential iteratively, giving us a more accurate potential each time and eventually converging to a solution. Note that we assume this process will converge but it is not explicitly obvious from the form of the potential that this will occur, and it is possible that with some initial conditions, the potential does not converge and instead swaps between some finite set of solutions. Regardless, initialised with either the 0 potential or the greens potential from before we do indeed converge to a solution. The code is ran such that it iterates the process from before with the Vdir potential instead and updates the 1s wavefunction each iteration, it then will break the loop in the difference in 1s energies is less than 10^{-6} . This is achieved via a while loop. The result of this is shown in the convergence of 1s energy in figure 7. We see that it converges to about 1.5 over 22 iterations. After the process has converged, we can measure quantities of interest such as binding energies, probability densities and lifetimes.

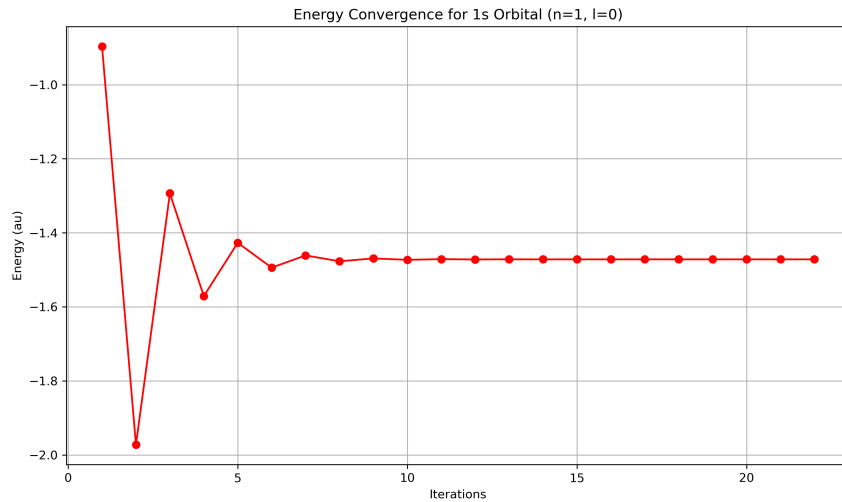


Figure 7: This graph tracks the energy convergence of the 1s orbital through multiple iterations. Starting with unstable values, the energy oscillates significantly in the first 5 iterations before steadily converging to approximately -1.5 au after 10 iterations. This demonstrates the iterative nature of the computational method and its eventual stability.

4.2 Binding Energies

To calculate the Binding Energies we use the same process as before where we extract and store the eigenvalue corresponding to the 2s and 2p energies. We plot this compared to experiment in figure 8. We can see that the energies are more accurate than the Green's potential but less accurate than the Green's potential with perturbation theory. This follows as we are using an iterative procedure to update the potential and making sure that our energies converge. However, it follows that our energies are less accurate than when we use perturbation theory as that also considers the direct potential indirectly in

the $\langle V_{ee} \rangle$ term as well as other effects.

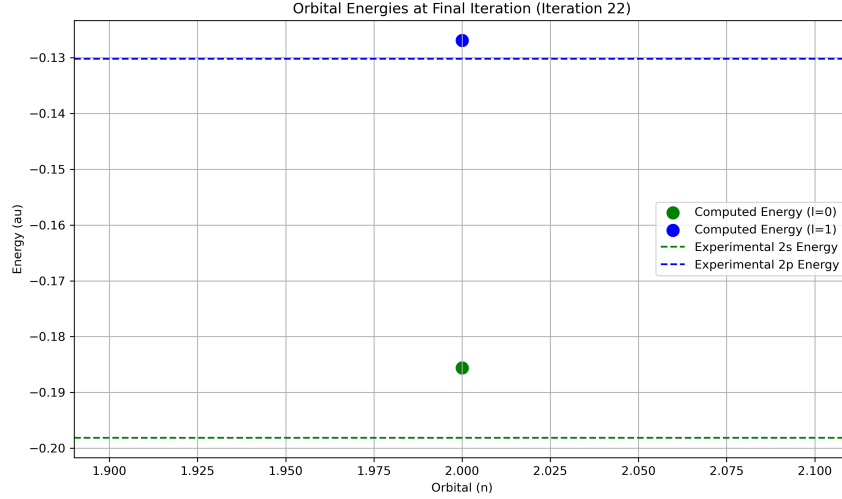


Figure 8: The final results after 22 iterations show computed energies (dots) versus experimental values (dashed lines). The green point shows the $l=0$ (2s) energy, close to but still slightly off from the experimental value. The blue point shows the $l=1$ (2p) energy, which matches well with the experimental value. This is clearly more accurate than the Green's potential but not as accurate as when we use perturbation theory.

4.3 Radial Probability Density

As with prior questions we can plot the radial probability densities for the 1s, 2s and 2p orbitals as shown in figure 9. We observe very similar probability densities as the Green's potential with the slight difference of the 2p state which is pushed slightly outwards and with a slightly reduced peak height. This means that our lifetime of the 2p state will also differ slightly, as it depends on the wavefunction of the 2s and 2p state.

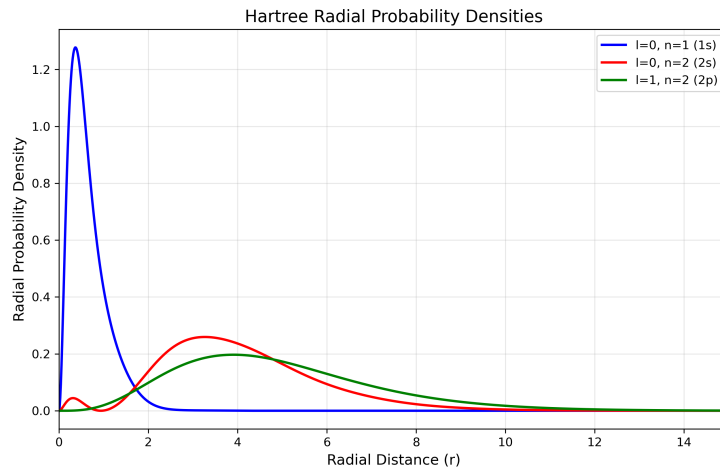


Figure 9: This plot shows the radial probability density distributions for lithium's orbitals using the Hartree method. We see a slight change from the Green's potential particularly in the 2p orbital.

4.4 Lifetime of 2p State

We find the Lifetime of the 2p state using the final iteration of the Hartree procedure with the 2s and 2p wavefunctions as we did previously and find

$$\tau_{2p} = 24.0333 \text{ ns}$$

which is far closer to the experimental value at 11.3% error. Which is more than twice as accurate as the Green's potential, indicating that the wavefunctions are more accurate. This suggests if we were to use perturbation theory on the green's potential for the wavefunctions, we could yield a more accurate lifetime with the simplified Green's model.

Regardless, the Hartree method clearly functions as expected and converges to a more accurate solution of the electron states than the Green's potential and suggests that the iterative method is useful to increase the accuracy of our solution.

5 B.4: Hartree-Fock

Recognising the use of the iterative method indicates that we should use a more accurate potential function by including an exchange component. This gives the full Hartree-Fock method where,

$$V_{\text{HF}} = V_{\text{dir}} + V_{\text{exch}}.$$

The exchange component isn't a function of r directly and instead we can only use its action on a radial wavefunction,

$$V_{\text{exch}}P_a(r) = - \sum_b^{\text{core}} 2(2l_b + 1) \sum_k \Lambda_{l_a, l_b}^k y_{b,a}^k(r) P_b(r),$$

where Λ is the angular coefficient ($\Lambda_{00}^0 = \frac{1}{2}$, and $\Lambda_{01}^1 = \frac{1}{6}$).

We only consider the valence s and p valence states which only gives us 2 cases to consider. We can hence modify our function which creates the Hamiltonian to include the exchange potential,

$$H_{ij} = \langle i | \hat{H}_r | j \rangle = \int b_i(r) \hat{H}_0 b_j(r) dr + \int b_i(r) \hat{V}_{\text{dir}} b_j(r) dr + \int b_i(r) \hat{V}_{\text{exch}} b_j(r) dr,$$

where

$$V_{\text{exch}} b_j(r) = -2\Lambda y_{1s, b_j}^k(r) P_{1s}(r).$$

We use this to iterate our potential and Hamiltonian by updating the 1s wavefunction each iteration as before. We begin by reading in the 1s wavefunction from the Hartree solution to speedup the process. Again we need to consider whether this process will converge or not and we find that it indeed does when our initial condition is the final solution from the Hartree procedure.

5.1 Convergence

We plot the energy of the 1s energy state in figure 10. We see that it requires far less iterations than the Hartree procedure but interestingly, the energy of the 1s state converges to ≈ -2.9 which is in strong disagreement with the Hartree procedure. This is because the deeply bound energy states are badly approximated by the Hartree procedure.

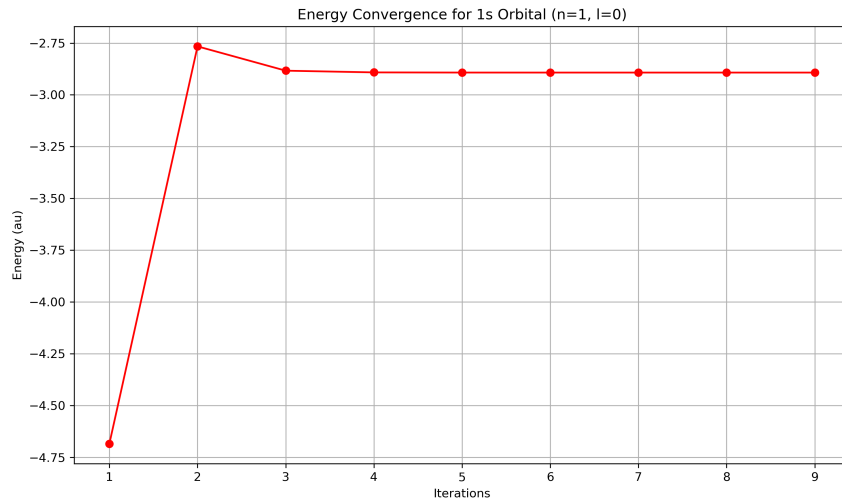


Figure 10: This graph tracks the iterative convergence of energy calculations for the 1s orbital using the Hartree method. Starting at a very low energy of approximately -4.7 au in the first iteration, the energy jumps dramatically to around -2.75 au by the second iteration, then stabilizes around -2.9 au by the third iteration. This is significantly different from the Hartree method despite initialised with the Hartree solution.

5.2 Binding Energies

When we calculate the Binding energies of the 2s and 2p we observe far closer alignment with experiment compared to previous approximations, including the greens potential with perturbation theory (fig. 11). This suggests that the full Hartree-Fock procedure is the most accurate method of simulation thus far.

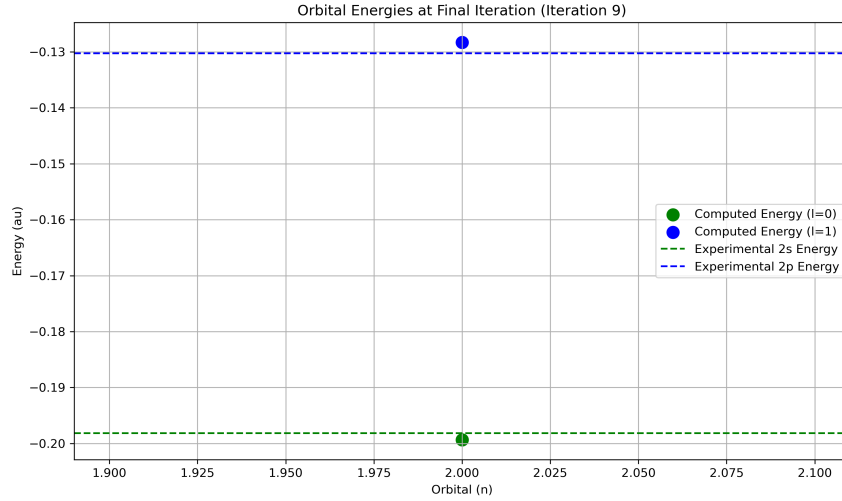


Figure 11: Energies for 2s and 2p orbitals using the HF method clearly showing us very accurate results for 2p and 2s. This has the most accurate values for 2s and close to the accuracy of Greens + Perturbation for 2p. This demonstrates that there is some advantage in the HF method.

5.3 Radial Wave Function

As with before we can calculate and plot the Radial wave functions and yield very similar results to prior sections with minor differences in the shape and peak of the distribution (fig. 12). We can use these distributions to find the lifetime of the 2p state.

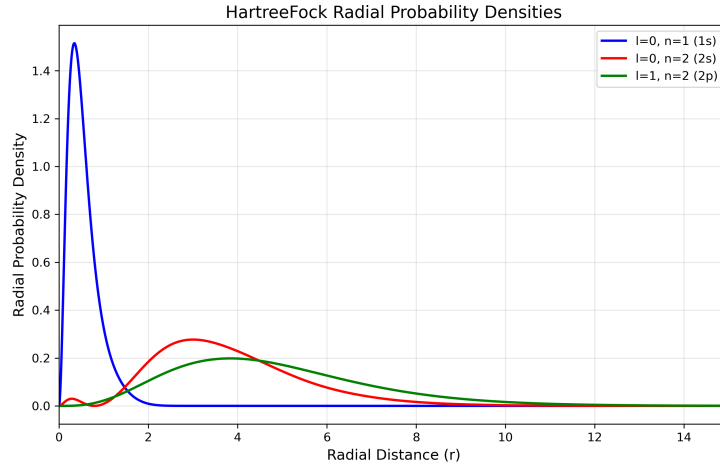


Figure 12: This graph depicts radial probability density functions for three different atomic orbitals calculated using the Hartree-Fock method. Again we see very similar results visually to the Hartree method but numerically we yield a far more accurate value for lifespan, indicating this is the most accurate probability density.

5.4 Lifetime of 2p State

We find the lifetime of the 2p state as 26.97 ns which is only 0.49% error compared to experiment, strongly within the 1% threshold we desired. This demonstrates that a Hartree-Fock method for iteratively updating the potential allows us to iteratively update the wavefunctions and achieve a highly accurate lifetime of the 2p state once the process converges. This is a substantial achievement considering the assumptions we made and the complexity of simulating a many body quantum system.

6 Approximations

The numerical approximations we make are based on the B-spline formalism. We choose B-splines of order 7 which means that we have the splines are polynomials of order 6. These splines allow us to have a complete basis for functions up to order 7. However, we are enforcing a few simplifying conditions. Firstly we have a finite number of B-splines which is

	Theoretical	Greens		Greens + Perturbation		Hartree		Hartree-Fock	
2s (au)	-0.19814	-0.16125	(18.6%)	-0.20616	(-4.0%)	-0.18558	(6.3%)	-0.19934	(-0.6%)
2p (au)	-0.13023	-0.12544	(3.7%)	-0.12919	(0.8%)	-0.12691	(2.6%)	-0.12829	(1.5%)
τ_{2p} (ns)	27.102	19.7726	(27%)	-	-	24.0333	(11.3%)	26.9700	(0.48%)

Table 1: Comparison of theoretical and computed values for 2s and 2p energy levels (in atomic units) and the 2p lifetime (in nanoseconds) using different computational methods: Greens function, Greens function with perturbation, Hartree, and Hartree-Fock. Percent deviations from the theoretical values are given in parentheses. The results indicate that the Hartree-Fock (HF) method provides the most accurate wavefunctions, leading to the best agreement for the 2s energy and 2p lifetime, while the Greens function with perturbation offers the best accuracy for the 2p energy.

an approximation for the basis, assuming that the higher order terms have vanishing coefficients. This appears to be a reasonable approximation given the results found, but for optimal results it is likely a larger value for N is required.

Additionally, we remove the first and last Bspline as they are not 0 at $r = 0, r_{max}$ which is the boundary condition for our $P(r)$ solutions. As such, we make our basis no longer complete for polynomials up to order 7 and instead approximately complete. This implies there is possibly some information around low and high r that is lost by our approximation.

Further, we remove the 2nd B-spline to improve numerical accuracy of our results as we expect the wave functions to act as a power law of r (r^l , $l \in \mathbb{R}^+$) at low r . The 2nd B-spline is too steep at low r and so removing it allows us to get more accurate results for our instance but again makes our approximation of a complete basis weaker.

Additionally, we can continue to use perturbation theory to get more accurate results and can use higher order perturbation theory to converge to experimentally matched results. This was not explored but is expected to yield good results as even the first order perturbation increased the accuracy of results substantially.

In terms of the problem formulation, there are 4 key assumptions we make that approximated away some of the higher order dynamics of the atom. Firstly, we consider only non-relativistic motion of the electrons and use the SE as a result. If we wanted more accurate results it is likely that a relativistic wave equation solution could improve our values. Secondly, we assume the nucleus has 0 volume as the potential is defined using the point charge assumption ($-Z/r$) which theoretically allows the electron to be inside the volume occupied by the nucleus. Removing this assumption would involve a more complex potential but may be more physically accurate. Thirdly, we could have used the reduced mass of the electron, μ , to account for the fact its orbit is around the joint centre of mass rather than just the centre of the nucleus. Lastly, we approximate the 1s orbital without considering the effects from higher order orbitals. If we wanted to model the 1s wavefunction and energy more accurately we could consider effects from higher order orbitals.

Finally, we have the largest assumption and approximation of this task which is the first order perturbation approximation of the mean field. Mathematically our Hamiltonian can be written as,

$$H = \sum_i^N \left(\frac{\mathbf{p}_i^2}{2} - \frac{Z}{|\mathbf{r}_i|} + u^{\text{MF}}(\mathbf{r}_i) \right) + \delta V, \quad \text{where} \quad \delta V = \sum_{i < j} \frac{1}{|\mathbf{r}_i - \mathbf{r}_j|} - \sum_i u^{\text{MF}}(\mathbf{r}_i).$$

If we assume δV to be small, it can be treated perturbatively, and we do so to first order. This is the mean field approximation (independent particle picture) which is the largest approximation we make for this project. This formalism is how we can use Green's approximation as well as the Hartree and Hartree Fock procedure. In future, one could try to treat the atom by considering each particle to be dependent but this will be very computationally expensive.

All such assumptions allowed the problem to be completed easier and using less intensive mathematics and still yielded accurate results so it is not needed for a project of this scale. However, for novel research applications or industry applications, if closer physical accuracy is required, such assumptions should be revisited and reevaluated.

7 Conclusion

Overall, we have used C++ to simulate a many body quantum system for the electron wavefunctions in a lithium atom. We built up our model using various assumptions. We began with a Coloumb potential to model a hydrogen-like lithium atom and compared to theory to test if our numerical simulations are accurate. We recover hydrogen like energy levels and wavefunctions. Next, we use a greens screening potential to model the electron-electron interaction and then apply a first order perturbation to correct the energy levels. We then calculate the lifetime of the 2p state to reasonable accuracy (27% error). We then implemented an iterative process (self consistent Hartree process) which uses the 1s wavefunction to update the direct potential each iteration. This converges our simulation to a more correct model of the atom resulting in an improved lifetime with 11.3% error. Finally, we added an exchange term in the Hamiltonian dependent on l which improves the accuracy of our model with a lifetime of 26.97 nanoseconds (0.48% error). In all, we demonstrated that numerical simulations of the lithium atom can be used to accurately model the electron wavefunctions, energies and then calculate the lifetime of the 2p state (our final results are presented in table 1). We do note however, there was sensitive dependence on the hyperparamaters of B-Spline number, order, number of data points, r_0 and r_{max} . Finally, all code is available on [Github](#).